Device-level Transient Cooling of β-Ga_2O_3 MOSFETs

Samuel H. Kim[1], James Spencer Lundh[2], Daniel Shoemaker[2], Bikramjit Chatterjee[1], Kelson D. Chabak[3], Andrew J. Green[3], Kyle Liddy[3], Samuel Graham[4], Sukwon Choi[2]*

[1]Georgia Institute of Technology, [2]The Pennsylvania State University, [3]Air Force Research Laboratory, [4]University of Maryland,

2022/06/03

2022 21st IEEE Intersociety Conference on Thermal and Thermomechanical Phenomena in Electronic Systems (iTherm)

1. Introduction
2. Device Description
3. Experimental and Modeling Details
4. Results and Discussion
5. Conclusion

WBG Semiconductor Device Applications

Power device operation: By switching a power device on periodically, current pulses are induced that allow for control circuits to be regulated.
RF device operation: An RF device or amplifier works at a constant DC bias, takes the low-power RF signal and amplify or convert it to a high-power signal.

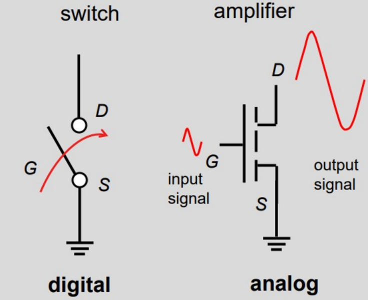

Ultra-Wide Bandgap (UWBG) Semiconductor β-Ga_2O_3

Table 1: Electronic and thermal properties of semiconductors used to construct radio frequency (RF) and power switching devices.

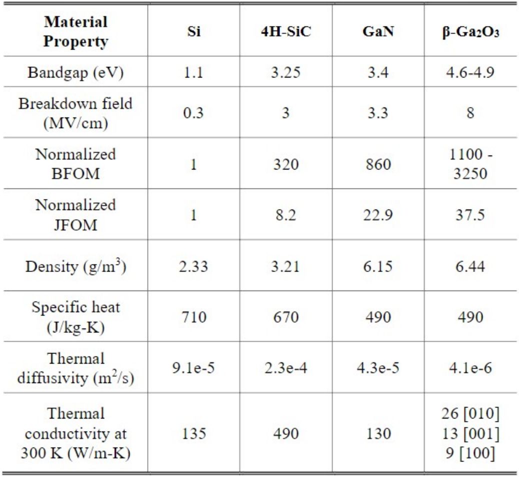

Material Property	**Si**	**4H-SiC**	**GaN**	**β-Ga_2O_3**
Bandgap (eV)	1.1	3.25	3.4	4.6-4.9
Breakdown field (MV/cm)	0.3	3	3.3	8
Normalized BFOM	1	320	860	1100 - 3250
Normalized JFOM	1	8.2	22.9	37.5
Density (g/m^3)	2.33	3.21	6.15	6.44
Specific heat (J/kg-K)	710	670	490	490
Thermal diffusivity (m^2/s)	9.1e-5	2.3e-4	4.3e-5	4.1e-6
Thermal conductivity at 300 K (W/m-K)	135	490	130	26 [010] 13 [001] 9 [100]

Transient Thermal Response of Power Device

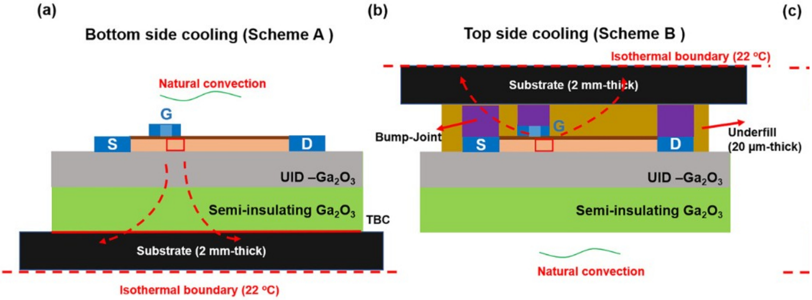

Figure 1: Schematic of heat transport path of different cooling schemes (a) bottom side cooling; (b) top side cooling.

Device thermal time constant (τ): the rise time for a device to reach $\sim 63\%$ of its steady-state temperature in response to a power step input.

$$\tau \propto 1/\alpha = \rho c_p / k$$

β-Ga_2O_3 Power Switching Device

Table 2: Thermal diffusivity of different semiconductor materials.

Material Property	Si	4 H−SiC	GaN	β-Ga_2O_3
α (m/s)	$9.1\mathrm{e}-5$	$2.3\mathrm{e}-4$	$4.3\mathrm{e}-5$	$4.1\mathrm{e}-6$

The heat diffusion length in β-Ga_2O_3 is limited under short transient thermal loading.

Therefore, device-level thermal management solutions established for GaN devices may not be applicable to β-Ga_2O_3 devices, especially under high frequency operating conditions that involve switching power losses.

β-Ga_2O_3 MOSFET

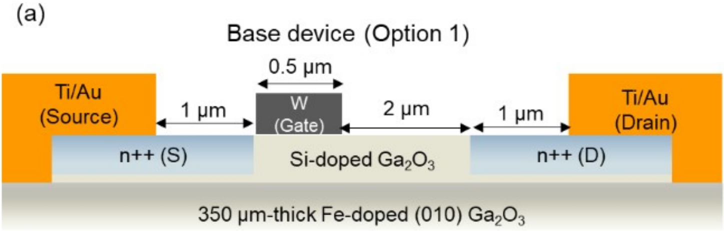

Figure 2: Schematic of a homoepitaxial β-Ga_2O_3 MOSFET.

A Si-doped β-Ga_2O_3 channel layer was grown on a Fe-doped (010)-oriented β-Ga_2O_3 commercial substrate using metal organic vapor phase epitaxy (MOVPE).

The channel length is 2.5 µm, where the gate length is 0.5 µm and the gate-drain length is 2 µm. The gate width is 100 µm.

Cooling Schemes

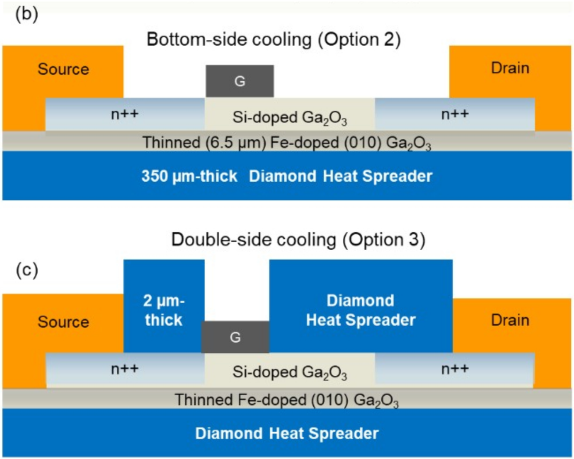

Figure 3: (b) bottom-side cooling; (c) double-side cooling, depositing a polycrystalline diamond heat spreader ouver the β-Ga_2O_3 channel layer.

GaN-on-Si HEMT

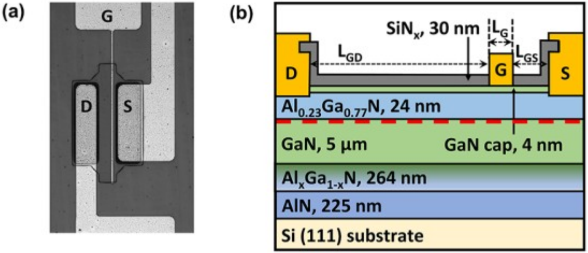

Figure 4: (a) Optical image of tested AlGaN/GaN HEMT; (b) Cross-sectional view of the HEMT.

The GaN HEMT has a 4.4 µm GaN buffer layer, a gate length of 2 µm, a gate width of 100 µm, a gate-to-source spacing of 2 µm,anda gate-to-drain spacing of 15 µm.

Transient Raman Thermometry

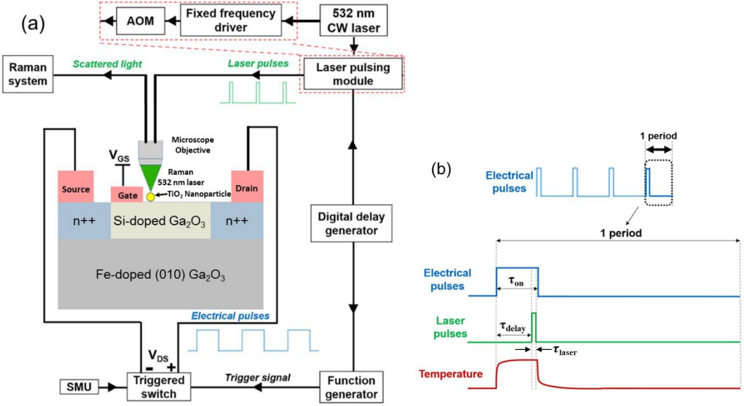

Figure 5: (a) Experimental setup (b) The synchronized pulsing scheme used to capture the transient thermal response.

A temporal resolution of 15 ns was achieved in this study.

The β-Ga_2O_3 MOSFET and GaN HEMT were operated under a fully open channel condition.

Modeling and Validation

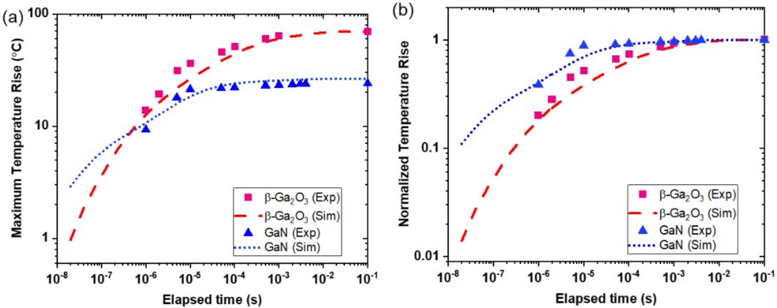

Figure 6: (a) Experimental data along with simulated results for the β-Ga_2O_3 MOSFET and GaN-on-Si HEMT that were operated under 1 W/mm and 1.6 W/mm, repectively. (b) Normalized temperature rise with respect to their steady-state temperature rise.

Modeling of Different Schemes

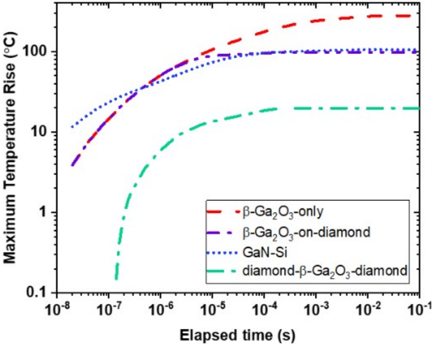

Figure 7: The transient channel temperature rise under a power density of 4 W/mm for a homoepitaxial β-Ga_2O_3 MOSFET with different cooling schemes and a GaN-on-Si HEMT.

A top-side heat spreader effectively reduces the temperature rise during short transient conditions (*e.g.*, $\Delta t < 10^{-5}\,\mathrm{s}$)

Conclusion

- Replacing the substrate with polycrystalline diamond could reduce the steady-state temperature rise by 65% compared to that for a homoepitaxial β-Ga_2O_3 MOSFET.
- However, for high frequency power switching applications beyond the $\sim 10^2$ kHz range, bottom-side cooling does not improvethe transient thermal response of the device.
- The use of a β-Ga_2O_3 composite substrate (bottom-side cooling) should be augmented by a diamond passivation layer (top-side cooling) to effectively cool the device active region under both steady-state and transient operating conditions.

Ultrafast Transient Heat Transport

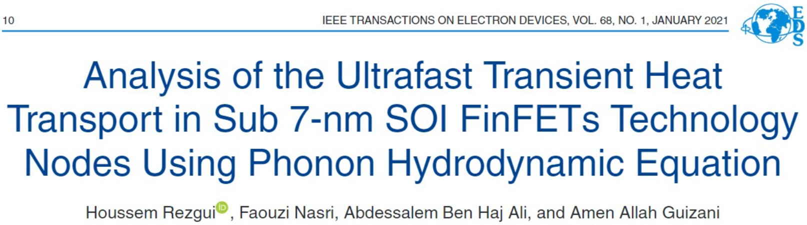

10 IEEE TRANSACTIONS ON ELECTRON DEVICES, VOL. 68, NO. 1, JANUARY 2021

Analysis of the Ultrafast Transient Heat Transport in Sub 7-nm SOI FinFETs Technology Nodes Using Phonon Hydrodynamic Equation

Houssem Rezgui, Faouzi Nasri, Abdessalem Ben Haj Ali, and Amen Allah Guizani

$$\frac{\partial T}{\partial t} + \tau_R \frac{\partial^2 T}{\partial t^2} - \frac{4}{15} l^2 \frac{\partial(\Delta T)}{\partial t} = \frac{1}{C} \nabla(\kappa \nabla T) + \frac{Q}{C}$$

$$T - T_W = -d_W \times l \times \frac{\partial T}{\partial x}$$

$$d_W = \frac{R_{\mathrm{TBR}} \times \kappa_{\mathrm{eff}}}{Kn \times L_h}$$

Ultrafast Transient Heat Transport

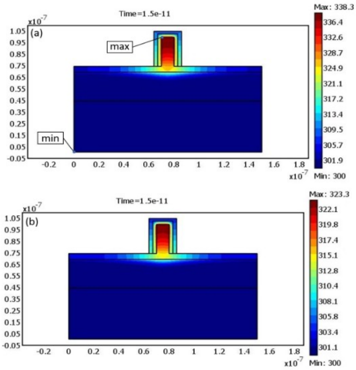

Fig. 7. Surface temperature distribution in the nanodevice at $t = 15$ ps for (a) $p = 0.1$ and (b) $p = 0.6$.

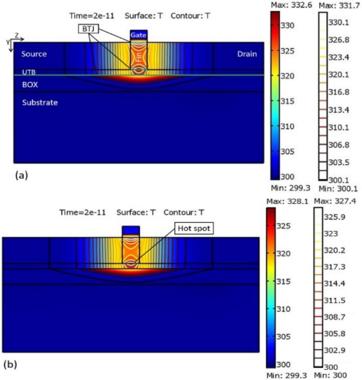

Fig. 8. 2-D Temperature maps from cross-sectional view at $t = 20$ ps for (a) $p = 0.1$ and (b) $p = 0.4$.

Thank You!